Received 1 November 2023; revised 25 January 2024; accepted 11 February 2024. Date of publication 14 February 2024; date of current version 26 March 2024.

Digital Object Identifier 10.1109/OJAP.2024.3366167

Reflectarray Antenna for Simultaneous Near-Field Fronthaul and Far-Field Backhaul Links in Next 5G FR2 Femtocells

ÁLVARO F. VAQUERO [1] (Member, IEEE), BORJA IMAZ-LUEJE [2] (Member, IEEE), MARCOS R. PINO [1], AND MANUEL ARREBOLA [1] (Senior Member, IEEE)

[1]Department of Electrical Engineering, Group of Signal Theory and Communications, Universidad de Oviedo, 33203 Gijon, Spain

[2]Department of Signal Theory and Communications and Telmatic Systems and Computing, Universidad Rey Juan Carlos, 28032 Madrid, Spain

CORRESPONDING AUTHOR: Á F. VAQUERO (e-mail: fernandezvalvaro@uniovi.es)

This work was supported in part by MCIN/AEI/10.13039/501100011033 under Project PID2020-114172RB-C21 (ENHANCE-5G), and in part by the Spanish Ministry of Universities and European Union (NextGenerationEU Fund) under Project MU-21-UP2021-03071895621J.

ABSTRACT This work presents a reflectarray-based base station antenna to integrate both backhaul (BH) and fronthaul (FH). The reflectarray operates at 28 GHz in dual linear polarization, using one polarization for the BH and another for the FH. The BH is a pencil beam of maximum gain pointing in a certain direction, while the FH defines the coverage for a femtocell. The FH is used to generate the coverage within the near field radiated by the base station. The synthesis of the FH is carried out by means of a near-field phase-only synthesis (NF-POS), while the BH is analytic. Both phase-shift distributions are physically implemented using a unit cell based on a double-layer topology of coplanar dipoles. The reflectarray is manufactured and evaluated in a spherical range (far field) and a planar range (near field). The measurements agree with the simulations, showing that a single antenna based on a reflectarray can be used to implement the dual link FH and BH.

INDEX TERMS Reflectarray antennas, base station, near field coverage.

I. INTRODUCTION

THE FIFTH Generation (5G) of mobile communications, as well as the next generation (Beyond 5G -B5G- and 6G) are boosting the use of millimeter-wave (mmWave) spectrum to provide broadband wireless access in cellular networks [1]. Those systems are expected to be deployed between 20 to 300 GHz, allowing for an increase in the data rate and system capacity or to decrease in latency concerning previous generations [2]. The bands such as 27, 39, and 60 GHz are being considered for the upcoming 5G, whilst higher frequencies over 100 GHz are being kept for B5G and 6G [3].

The use of mmWave spectrum in communications has raised new challenges related to signal propagation conditions. A higher frequency leads to a more rapid attenuation (path loss is increased) and a higher sensitivity to physical barrier, due to penetration losses are also larger [4]. The coverage generated by a base station (BS) might be disrupted by high-density areas of buildings in outdoor scenarios (streets), while indoor coverage (shopping malls, airports, offices, etc.) might be affected by different elements, such as walls or furniture. Those effects result in areas with poor or even null coverage, which are so-called blind zones.

Radio-frequency boosters could be used to extend the cellular coverage in those areas [4]. However, this approach would significantly increase the costs of the network infrastructure, and complexity and produce interference with other systems. A less complex and low-cost solution is to deploy femtocell BS whose radiation is adapted to the blind zone. Therefore, the BS would generate a fronthaul (FH) covering the blind zone. However, these BSs are still needed for a high-capacity backhaul (BH), which is typically based on wired solutions (i.e., optic fiber), resulting in a costly deployment.

In this work, a reflectarray-based BS is proposed as an alternative to deploying femtocells, obtaining a

single-antenna topology to generate both BH and FH links at Ka-band. Reflectarray (RA) antennas have been an attractive solution in several applications, especially in communication systems [5], [6]. RA provides a low-profile, low-visual-impact, low-cost, and easily manufactured process antenna with beam shaping capabilities (which is a main advantage to reach a customizable radiation pattern). In recent years, RA has caught the attention in 5G communication in the mmWave to be used as Reflective Intelligent Surfaces (RIS) [7], [8], [9]. However, RIS only tilts the FH link. The proposed RA is designed to radiate a shaped pattern to perform the coverage, which is within the near field region (considering the distance with users and the antenna aperture size in a femtocell) [10]. Then, the RA radiates a pencil beam pointing to another BS, thus enabling the BH link. To simultaneously deploy both links, the RA works in dual-linear polarization. The FH coverage is reached through a Near-Field Phase-Only Synthesis (NF-POS), while the BH is analytic. The unit cell is a dual layer set of orthogonal dipoles, which provides independent control of each polarization and high isolation between orthogonal polarizations. The RA is manufactured and evaluated in an anechoic chamber and a planar acquisition range to obtain a full characterization of the radiation pattern of the antenna. The measurements highly agree with the simulations, obtaining a successful implementation of a reflectarray-based BS to reach a FH/BH link at Ka-band. Moreover, to the best aware of the authors, this is the first prototype with far and near field constraints, considering that the near field specifications are not a focus beam but a shaped one. The proof of concept presented in this work can be extended from dual-linear to dual-circular polarized antenna (each polarization for BH and FH, respectively) using a proper unit cell and a dual-circularly-polarized feed to ensure the connectivity of the BS in both links. Although mm-Wave 5G communication requires to use dual-linear polarization (either $\pm 45^\circ$ or V/H) to apply MIMO techniques [11], [12], this work is focused on near-field indoor applications that does not require polarization diversity.

II. ANTENNA DESIGN

A. ANTENNA OPTICS AND UNIT CELL

The reflectarray is comprised of 44×44 elements distributed in a regular grid of periodicity $0.4\lambda\times0.4\lambda$ (4.29 mm $\times$ 4.29 mm) at 28 GHz. The aperture size is about 190 mm$\times$190 mm and the feed is placed at $\vec{r}_f = (79.4,\ 0,\ 200)$ mm according to the system of coordinates shown in Figure 1. Thus, the f/D is 0.97. The feed is a horn antenna of 20 dBi gain at 28 GHz that provides an incident field with an illumination taper of 16 dB in both polarizations.

The unit cell is a dual-layer topology based on sets of orthogonal coplanar dipoles [13]. The unit cell and its geometrical parameters are shown in Figure 2. The three parallel dipoles oriented to the X-axis (top layer) and the one in the bottom layer control the response of the V-polarization

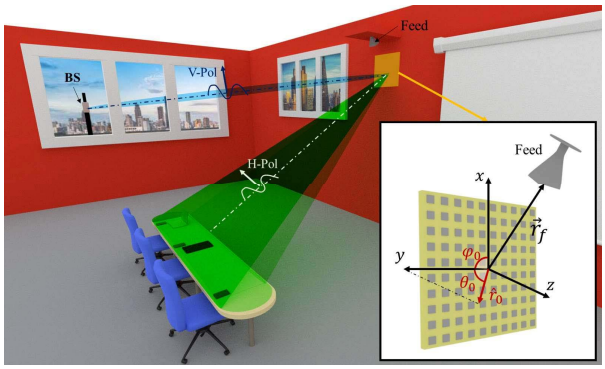

FIGURE 1. Sketch of a 5G scenario to use the base station with integrated fronthaul (H-polarization) and backhaul (V-polarization).

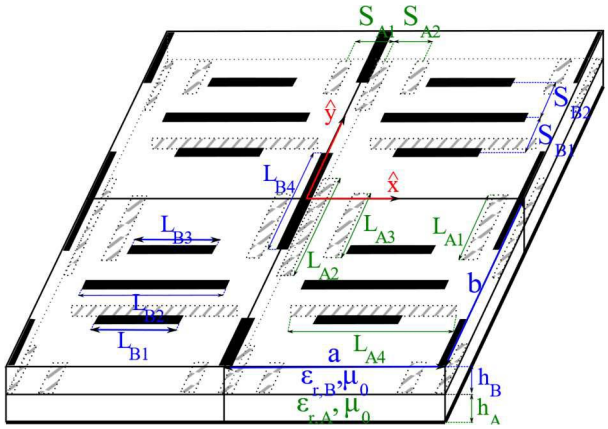

FIGURE 2. Geometry of the unit cell based on two sets of orthogonal coplanar dipoles.

(BH link). The three dipoles (bottom layer) and the one on the top layer oriented to the Y-axis control the H-polarization (FH coverage). The dipoles are printed in a dielectric layer of RT/Duroid 5880 ($\epsilon_r = 2.3, \tan\delta = 0.0013$) of height ($h_A$ and h_B) 30 mils. The geometrical parameters shown in Figure 2 are adjusted to obtain a smooth and linear phase response. In particular, the length of the central dipole L_{A2} is used to control the phase response since the other dipoles are related to this dipole length by the factors: $\alpha_{A1} - \alpha_{A4}$ and $\alpha_{B1} - \alpha_{B4}$ as Table 1 shown. Moreover, the width of the dipoles is 0.38 mm and its separation (S_{A1}, S_{A2}, S_{B1} and S_{B2}) 0.78 mm. The scale factors and the other geometrical parameters have been optimized to find the best unit cell response using previous works as reference [14]. The analysis of the unit cell is performed by using an in-house electromagnetic code based on the Method of Moments in Spectral Domain (MoM-SD) [15]. The analysis is carried out under a periodic environment, and basis functions accounting for edge singularities are used in the approximation of the current density of the dipoles [15]. Figure 3 shows the response of the cell considering normal and oblique incidence for different angles ($\theta = 15^\circ,\ \varphi = 20^\circ$; $\theta = 30^\circ, \varphi = 40^\circ$). The unit cell provides a phase shift range up to more than a phase cycle in both polarizations,

TABLE 1. Relation of the geometrical parameters of the unit cell.

Parameter	Value
$\alpha_{A1} = L_{A1}/L_{A2}$	0.48
$\alpha_{A3} = L_{A3}/L_{A2}$	0.48
$\alpha_{A4} = L_{A4}/L_{B2}$	1.00
$\alpha_{B1} = L_{B1}/L_{B2}$	0.43
$\alpha_{B3} = L_{B3}/L_{B2}$	0.43
$\alpha_{B4} = L_{B4}/L_{A2}$	0.92

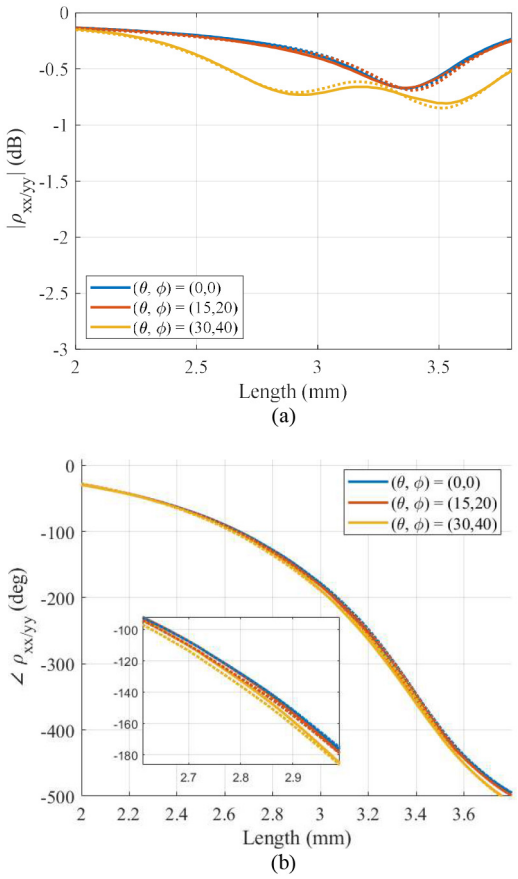

FIGURE 3. Amplitude (a) and phase (b) response of the proposed unit cell according to the variation of the length of the central dipole at 28 GHz and different angles of incidences. V-pol. (ρ_{xx}) in solid line and H-pol. (ρ_{yy}) in dotted line.

and a stable response in oblique incidence. Besides, the unit-cell losses are lower than 0.8 dB for most of the incidence θ. As a result, the unit-cell exhibit good angular stability.

B. SCENARIO REQUIREMENTS

The reflectarray works in dual polarization, using the *V*-polarization for the BH link and the *H*-polarization for the FH. The FH must cover a blind area defined within the near field of the reflectarray. The reflectarray is placed at a height of 2.5 m from the floor (see Figure 1), and the coverage is generated in a corridor (indoor) or street (outdoor) scenario. The coverage is defined in a range of 1.2 m × 0.4 m, which is equivalent to a 585% and 195% of the aperture of the antenna in the *z*- and *y*- direction, respectively. Within this area the field should be as uniform as possible, setting a maximum ripple of 3 dB. Outside the coverage the field should rapidly decrease to avoid radiation in undesired directions. Thus, the minimum difference between the field within the coverage and outside must be −12 dB.

The BH is defined as a point-to-point link connecting the reflectarray with another external base station. To reach the maximum efficiency in the link the reflectarray generates a beam with its maximum gain in the direction (θ_0, φ_0) (direction in which the external BS is located).

C. DESIGN PROCEDURE

The design of the reflectarray is based on an independent procedure for each polarization. The FH requires a shaped near field pattern tailoring the coverage, so the design is carried out through a NF-POS using the generalized Intersection Approach algorithm [16]. In this case, the constraints are imposed on the amplitude of the radiated near field. As a starting point for the NF-POS, the phase-shift distribution used is associated with a beam focused on the center of the coverage (1) [17]. The synthesis is carried out following a multi-stage process, which is based on dividing the synthesis into multiple stages whose goal is finding out an intermediate solution [18]. When carrying out synthesis, especially in near field with complex specifications that are far from the starting point, it is necessary to subdivide the synthesis process into several synthesis to enhance the convergence of the algorithm. Instead of attempting a single-stage synthesis starting from the starting point given by (1) in this case and trying to directly find a solution that meets the specifications, the process is divided into several stages (or syntheses). In each synthesis, the goal is finding a different intermediate solution. Initially, an intermediate solution is defined as a solution close to the starting point, for instance, by allowing more ripple or soughing for a field distribution in a smaller area. As these intermediate solutions are achieved, complexity and solution requirements will gradually increase until the desired specifications are ultimately met.

$$\phi(x_l, y_l) = -\frac{2\pi}{\lambda_0}\left(\left\| \vec{r}_{NFF} - \vec{r}_l \right\|_2 - d_{fl}\right) \tag{1}$$

where λ_0 is the wavelength at the central frequency, d_{fl} is the distance from the feed to the lth element, $\vec{r}_{NFF} = (x_{NFF}, y_{NFF}, z_{NFF}) = (-1.6,\ 0,\ 1.5)$ m is the point at which the near field is focused, and $\vec{r}_l = (x_l, y_l, 0)$ is the position vector of the lth element.

The output of the synthesis process is the phase-shift distribution depicted in Figure 4(a). It is the phase of the reflection coefficients in the *H*-polarization (ρ_{yy}) to be applied to each element to generate the required radiated near field.

Figure 5(a) shows the results of the NF-POS, achieving compliance with the requirement of 90% (considering the 3 dB ripple specification). Moreover, the field rapidly decays beyond the coverage, satisfying the minimum difference of 12 dB set in this area.

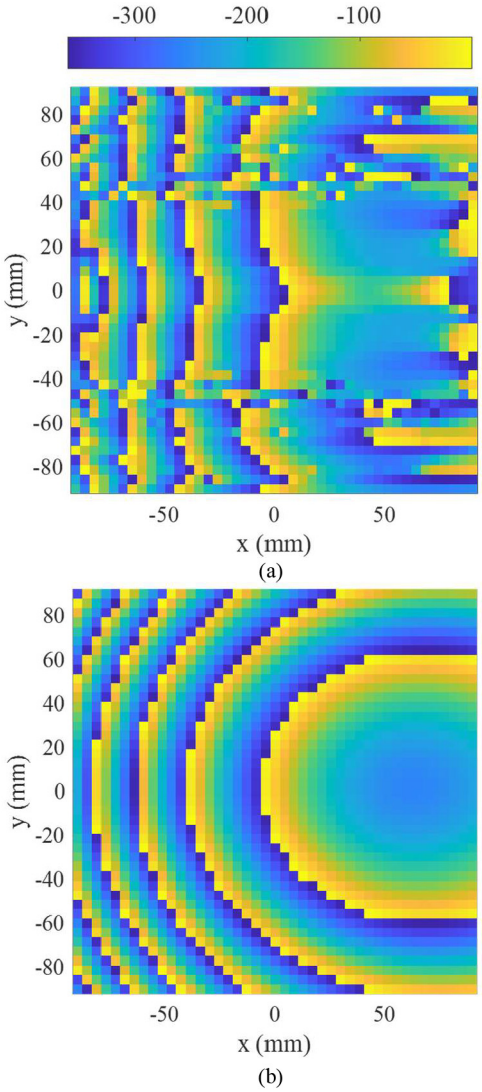

FIGURE 4. Phase distribution in degrees [°] required in each polarization of the design: (a) Phase for the H-polarization to collimate a NF coverage; (b) phase for the V-polarization to generate a pencil beam pattern.

In the case of the BH, a high-gain pencil beam is required in X polarization. The phase distribution (ρ_{xx}) is analytically computed with (2), which is based on geometrical optics.

$$\phi(x_l,\ y_l) = k_0\big(d_{fl} - (x_l\cos\varphi_0 + y_l\sin\varphi_0)\sin\theta_0\big), \qquad (2)$$

where k_0 is the wavenumber in vacuum, and (θ_0, φ_0) are the pointing direction of the pencil beam, in this case 20.5° and −103°, respectively. This corresponds with a down tilt of 5° in elevation and a tilt of 20° in azimuth plane. Figure 4(b) provides the phase-shift distribution computed with (2).

Once both phase-shift distributions are obtained, the elements of the reflectarray are designed. In the design process, the length of the dipoles L_{A1}, L_{A2}, L_{A3}, L_{A4}, L_{B1}, L_{B2}, L_{B3} and L_{B4} are adjusted to produce both phase shifts in X and Y polarizations previously obtained. The design is carried out element-by-element, considering the real angle of incidence and the real incident field generated by the primary feed. In the design process, the same in-house MoM-SD is used again. The output of this process is the layout of 44 × 44 cells for the reflectarray.

III. EXPERIMENTAL VALIDATION

The designed layout is manufactured and measured in the facilities of Universidad de Oviedo to obtain a whole characterization of the FH and BH link.

A. FRONTHAUL COVERAGE

The field radiated by the reflectarray is first measured in a near-field planar acquisition range to evaluate the FH coverage [19]. Due to the physical dimension of the planar acquisition range (1.5 m × 1.5 m × 1.5 m), the measurements are divided into two steps. The field is measured at 500 mm from the center of the reflectarray in a regular grid of 800 × 500 mm^2 and parallel to the antenna aperture. This grid ensures that most of the radiated power (over a 90%) is captured. Then, the field at the coverage is obtained through a Near Field to Near Field (NF-NF) transformation using the tool GRASP [20]. This two-step measurement has been demonstrated in previous works [21].

Figure 5 shows the near field pattern at 28 GHz after the NF-NF transformation at the coverage. The copolar (CO-Pol) component is defined as the component parallel to the H-polarization (Y-polarization) of the reflectarray, while the cross-polar (XP-Pol) is defined according to the V-polarization (X-polarization). The CO-Pol is similar to the one obtained after the POS (see Figure 5) resulting in a pattern that is adapter to the rectangular shape of the coverage. The coverage is slightly narrower than the synthesized results in the **z**-direction. However, the ripple is quite uniform in most of the area, obtaining compliance over a 82% for a 3 dB ripple. If the compliance is computed for a 4.5 dB ripple, it increases up to 96.77%. Therefore, the total whole area is near to satisfying the specifications. The XP presents a significantly low level, reaching a CO/XP-Pol minimum of 34 dB in the coverage. Thus, there is high isolation between polarizations.

B. BACKHAUL COVERAGE

Second, the reflectarray is also measured in a spherical acquisition range in an anechoic chamber to obtain the radiation pattern of the antenna and therefore evaluate the performance of the BH beam, as shown in Figure 6. The distance between the Antenna Under Test (AUT) and the probe is 5 m. Thus, owing to the antenna aperture, the acquisition is carried out in the Fresnel zone of the antenna and a Near Field to Far Field (NF-FF) transformation is applied by using SNIFT software [22].

Figure 7 presents the radiation pattern in terms of the CO-Pol and XP-Pol components at 28 GHz for the V-polarization. The beam points to the desired direction ($u = -0.08$, $v = -0.34$) having a peak gain of 31.36 dBi. This small difference in the **u**-direction is associated with mechanical tolerances of the measuring system and antenna

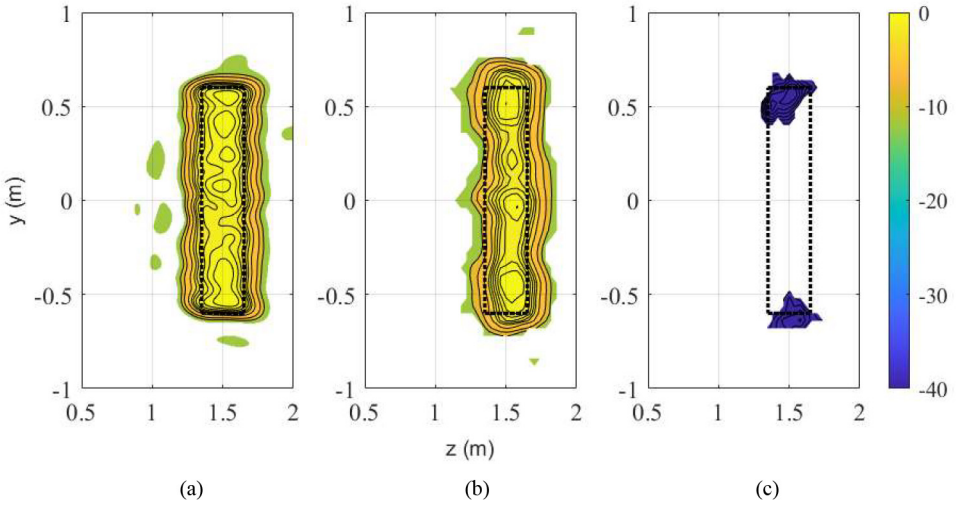

FIGURE 5. Simulated copolar (a) measured copolar (b) and cross-polar (c) component (dB) of the near field pattern at the FH coverage for the H-polarization at 28 GHz.

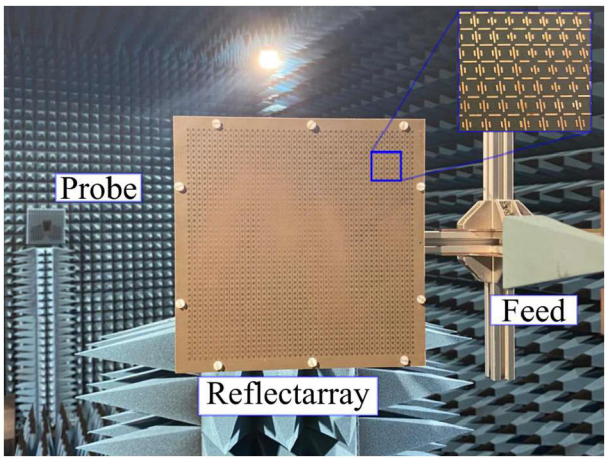

FIGURE 6. Set-up at the spherical anechoic chamber at Universidad de Oviedo to evaluate the radiation of the BH link.

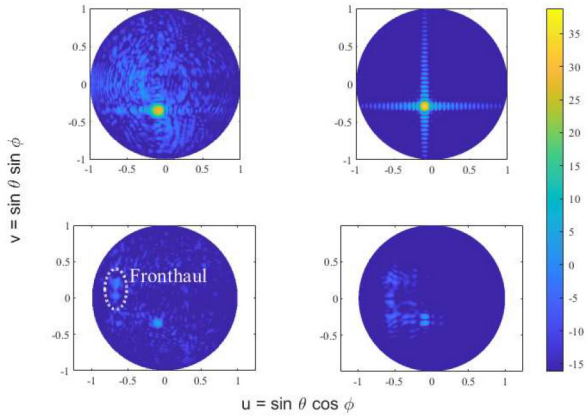

FIGURE 7. Comparison between measurements (left) and simulations (right) of the copolar (up) and cross-polar (bottom) component of the radiation pattern in dB of the BH link for the V-polarization at 28 GHz.

assembly. Besides, there is no radiation in other directions enhancing the performance of the BH link. The maximum of the XP-Pol is reached in two areas. First, the XP-Pol is expected in the direction of the pencil beam. Second, the one generated in the near field coverage. Both cases present an XPD (cross-polar discrimination) higher than 30 dB, so the isolation between the two linear polarizations is high.

Table 2 provides the gain budget analysis in the far-field operation of the antenna. The directivity is computed considering a uniform illumination of the reflectarray aperture [23]. The small spillover losses are due to the lower illumination in the reflectarray edges, as mentioned in Section II-A. The gain predicted after the analysis is slightly higher than the measured one. This difference is associated with two factors. First, there is a difference of almost 1 dB between the gain considered in the feed used in the analysis ($\cos\theta$ function) and the full wave simulated feed. Second, the uncertainty of the SGH used in the intercomparison gain measurement may be slightly higher up to ± 0.5 dB.

TABLE 2. Gain budget analysis of the reflectarray for the backhaul (BH) link (V-pol) at 28 GHz.

Parameter	Value
Directivity [dBi]	**35.91**
Spillover loss [dB]	-0.03
Aperture taper loss [dB]	-1.59
Average dielectric loss [dB]	-0.48
Average cross-polar loss [dB]	-0.78
Feed mismatch loss [dB]	-0.18
Total loss [dB]	**-3.00**
Gain predicted [dBi]	**32.91**
Gain measured [dBi]	**31.36**

C. IN-BAND PERFORMANCE

The performance of both links has also been measured the frequency band associated with the 5G channel n261, which covers frequencies from 27.50 to 28.35 GHz. Figure 8 shows the coverage obtained for the FH at different frequencies

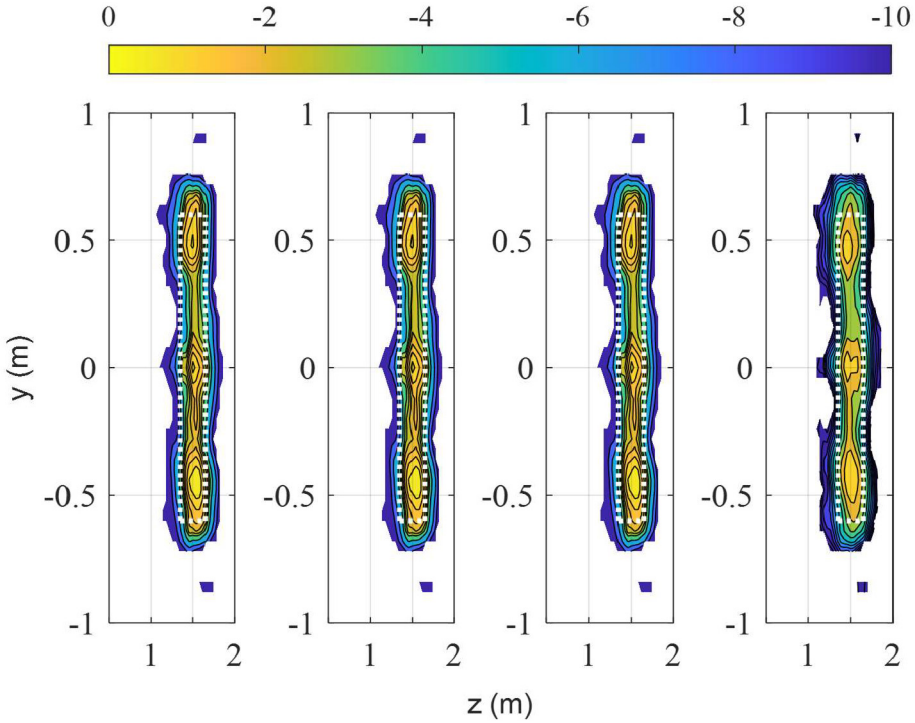

FIGURE 8. Measured in-band CO response (dB) of the coverage generated for the FH link (H-pol.). From left to right: 27.50, 27.75, 28 and 28.35 GHz. The field lower than −12 dB is not plotted.

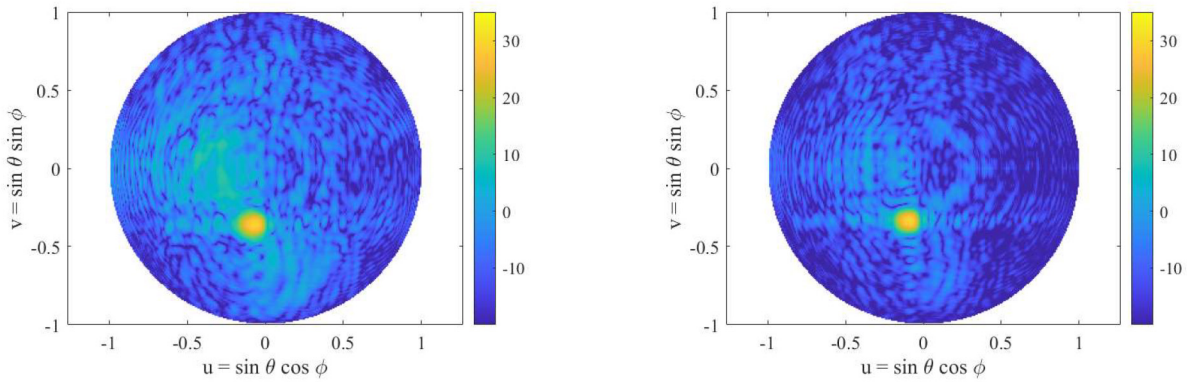

FIGURE 9. Measured in-band CO-Pol response (dBi) of the BH link (V-pol.) at (a) 27 (b) 29 GHz.

TABLE 3. In-band response of the reflectarray for the fronthaul (FH) link (H-pol.) within the 5G *n*261 channel.

Frequency (GHz)	Ripple 3 dB (%)	Ripple 4.5 dB (%)	CP/XP (dB)
27.50	74.65	94.93	34.14
27.75	74.75	94.93	34.18
28.00	82.00	94.00	34.22
28.35	83.41	96.77	37.42

TABLE 4. In-band response of the reflectarray for the backhaul (BH) link (V-pol.) from 27 to 29 GHz.

Frequency (GHz)	Gain (dBi)	CP/XP (dB)	Pointing Direction (u, v)	(θ_0, φ_0)
27	29.74	25.96	(-0.07, -0.36)	(21.5°, −101°)
28	31.36	24.27	(-0.08, -0.34)	(20.5°, −103°)
29	31.51	22.78	(-0.09, -0.34)	(20.6°, −105°)

within the channel (27.50, 27.75, 28 and 28.35 GHz). The result is a very stable coverage area within this band, reaching very uniform field distribution with a low ripple. Table 3 summarizes the compliance evaluated for maximum ripple of 3 and 4.5 dB. In the case of lower frequencies, the ripple increases a little, but observing the compliance at 4.5 dB, it can be concluded that the deviation is minimal. However, in all the cases is over 74% and 94% for 3 and

TABLE 5. Comparison of different arrays and reflectarrays for far- and near-filed application.

Ref.	Cell		Size [λ_0]	Field Pattern		Frequency Band (f_0 GHz)	Polarization
	Topology	Number of layers		Near Field	Far Field (Gain)		
[24]	Microstrip square patches	1	11 x 11	Multiple near-field focus	Pencil beam (N.A.)	Ku (16.0)	Dual-linear
[25]	Sets orthogonal coplanar dipoles	1	32 x 32	Shaped pattern with amplitude constraints	-	K (24.1)	Dual-linear
[26]	Sets orthogonal coplanar dipoles	1	18 x 18	Shaped pattern with amplitude and phase constraints	-	Ka (28.0)	Dual-linear
[27]	Fractal patches	1	8 x 8 9 x 9	-	Pencil beam 22.9 dBi* Pencil beam 25.7 dBi*	Ka (27.0) Ka (32.0)	Dual-linear
[28]	Stacked Variable Size Patches	2	15 x 15	-	El: Cosecant-Squared Az: Sectorial (20 dBi)	K (25.5)	Dual-linear
This work	Sets orthogonal coplanar dipoles	2	18 x 18	Shaped pattern with amplitude constraints	Pencil beam (31.36 dBi)	Ka (28.0)	Dual-linear

*Values obtained in simulations.

4.5 dB ripple, respectively. Besides, as shown in Figure 5 at central frequency, the compliance is affected by the corner areas where the field is forced to adjust to very tight angles. However, the field maintains a very uniform distribution throughout the central area coverage.

For simplicity the XP-Pol is not depicted, but similar levels are obtained within the band, reaching a very high crosspolar discrimination. The minimum CO/XP -Pol is over 34 dB, see Figure 5 and Table 3.

The antenna has been also measured at 27 and 29 GHz to evaluate the BH link. Figure 9 shows the radiation pattern for the copolar component at these two frequencies. In this case, directional beams similar to those obtained at the design frequency are obtained. Table 4 shows in more detail the values of gain, CO/XP -Pol and pointing direction obtained, as well as Figure 10 that compares the expected gain with the measured one. For this last comparison the measured gain has been obtained by a gain comparison method, which establishes an uncertainty of 0.25 dB due to the probe used. The gain is very stable, 29.74 at 27 GHz a maximum of 31.36 dBi at 28 GHz. Moreover, within this band the CO/XP -Pol ratio is always better than 22 dB, which results in a good isolation between the two polarizations. The CO/XP -Pol is computed considering the maximum of the XP-Pol, regardless of whether it is in the BH or FH area.

The beam squint has also been evaluated since the pointing direction changes due to frequency variation. Although there is a displacement in the pointing direction, it hardly changes within this 2 GHz. Therefore, the BH link is maintained from 27 to 29 GHz, which perfectly covers the n265 channel.

D. COMPARISON WITH OTHER WORKS

Table 5 lists some arrays and reflectarrays reported in the literature. To the best of the author's knowledge, this is the first reflectarray approach that operates both in near- and far-field. Array antennas have been proposed to operate near- and far-field simultaneously as stated in [24]. However, the presented reflectarray does not generate focused spots as in [24] but a shaped near-field beam adjusted to a complex coverage.

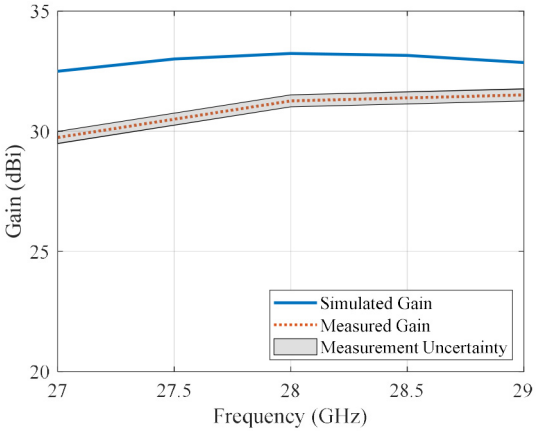

FIGURE 10. Comparison between the measured and simulated gain (dBi) in the entire band for the fronthaul link. The measured gain considers an uncertainty of ±0.25 *dB*.

In comparison to other works involving reflectarrays, the proposed antenna uses a cell topology akin to the one reported in [25] and [26]. It generates a shaped beam similar to [25] in near-field, and a high-gain pencil-beam as the reflectarray reported in [27]. Furthermore, the proposed reflectarray concept can be extended to generate other shaped beam patterns, both in near- and far-field, such as the ones outlined in [26] and [28].

IV. CONCLUSION

This work demonstrates the feasibility a reflectarray antenna to generate simultaneous backhaul and fronthaul links when it is used in base station for 5G FR2 femtocells. The antenna is designed to consider far field constraints for the backhaul and a fronthaul with near field constraints. The

design for the fronthaul is carried out by means of a Phase-Only Synthesis since a shaped near field pattern is required, while the backhaul can be obtained by means of geometrical optics equations. To integrate both designs into a single antenna, the unit cell is based on a dual-layer dielectric with sets of coplanar and orthogonal dipoles. This unit cell allows an independent control of each linear polarization and a high isolation between polarizations. The antenna is manufactured and measured to evaluate the radiation of both polarizations. The measurements show a high agreement with the simulations, not only validating the design procedure but also the control of the radiation of a near field and far field beam. Moreover, this is the first prototype evaluated for a simultaneously shaped beam near field pattern and a far field radiation pattern. The technique presented in this work can be extended to the use of a dual circular polarization antenna (each polarization for BH and FH, respectively), using a proper reflectarray cell and a dual-circularly-polarized feed. The antenna ensures the connectivity of the base station in both links. Moreover, this antenna is proposed for near-field indoor scenarios, which does not require polarization diversity for being used in MIMO.

REFERENCES

[1] T. S. Rappaport, Y. Xing, G. R. MacCartney, A. F. Molisch, E. Mellios, and J. Zhang, "Overview of millimeter wave communications for fifth-generation (5G) wireless networks with a focus on propagation models," *IEEE Trans. Antennas Propag.*, vol. 65, no. 12, pp. 6213–6230, Dec. 2017.

[2] W. Hong et al., "The role of millimeter-wave technologies in 5G/6G wireless communications," in *IEEE J. Microw.*, vol. 1, no. 1, pp. 101–102, Jan. 2021.

[3] T. S. Rappaport et al., "Millimeter wave mobile communications for 5G cellular: It will work!," *IEEE Access*, vol. 1, pp. 335–349, 2013.

[4] M. Shafi et al., "Microwave vs. millimeter-wave propagation channels: Key difference and impact on 5G cellular systems," *IEEE Commun. Mag.*, vol. 56, no. 12, pp. 14–20, Dec. 2018.

[5] D. Martinez-De-Rioja, E. Martinez-De-Rioja, J. A. Encinar, R. Florencio, and G. Toso, "Reflectarray to generate four adjacent beams per feed for multispot satellite antennas," *IEEE Trans. Antennas Propag.*, vol. 67, no. 2, pp. 1265–1269, Feb. 2019.

[6] M. Zhou, S. B. Sorensen, O. S. Kim, E. Jorgensen, P. Meincke, and O. Breinbjerg, "Direct optimization of printed reflectarray for contoured beam satellite antenna applications," *IEEE Trans. Antennas Propag.*, vol. 61, no. 4, pp. 1995–2004, Apr. 2013.

[7] E. Martinez-De-Rioja, Á. F. Vaquero, M. Arrebola, E. Carrasco, J. A. Encinar, and M. Achour, "Passive dual-polarized shaped-beam reflectarrays to improve coverage in millimeter-wave 5G networks," in *Proc. 15th Eur. Conf. Antennas Propag. (EuCAP)*, 2021, pp. 1–5.

[8] D. Martinez-De-Rioja, J. A. Encinar, E. Martinez-De-Rioja, Á. F. Vaquero, and M. Arrebola, "A simple beamforming technique for intelligent reflecting surface in 5G scenarios," in *Proc. Int. Workshop Antennas Technol. (iWAT)*, 2022, pp. 249–252.

[9] Á. F. Vaquero et al., "Reflectarray-based intelligent reflecting surface to improve mm-Wave 5G coverage in outdoor scenarios," in *Proc. IEEE Int. Symp. Antennas Propag. USNC-URSI Radio Sci. Meet. (AP-S/URSI)*, 2022, pp. 794–795.

[10] B. Imaz-Lueje, Á. F. Vaquero, D. R. Prado, M. R. Pino, and M. Arrebola, "Shaped-pattern reflectarray antennas for mm-Wave networks using a simple cell topology," *IEEE Access*, vol. 10, pp. 12580–12591, 2022.

[11] O. Jo, J.-J. Kim, J. Yoon, D. Choi, and W. Hong, "Exploitation of dual-polarization diversity for 5G millimeter-wave MIMO beamforming systems," *IEEE Trans. Antennas Propag.*, vol. 65, no. 12, pp. 6646–6655, Dec. 2017.

[12] A. Simonsson, S. O. Petersson, and G. Widell, "Dual polarization beamforming coverage demonstrated with 5G NR SSB," in *Proc. IEEE 32nd Annu. Int. Symp. Pers., Indoor Mobile Radio Commun. (PIMRC)*, Helsinki, Finland, 2021, pp. 800–804.

[13] R. Florencio, J. A. Encinar, R. R. Boix, V. Losada, and G. Toso, "Reflectarray antennas for dual polarization and broadband telecom satellite applications," *IEEE Trans. Antennas Propag.*, vol. 63, no. 4, pp. 1234–1246, Apr. 2015.

[14] D. R. Prado et al., "Efficient crosspolar optimization of shaped-beam dual-polarized reflectarrays using full-wave analysis for the antenna element characterization," *IEEE Trans. Antennas Propag.*, vol. 65, no. 2, pp. 623–635, Feb. 2017.

[15] R. Florencio, R. R. Boix, E. Carrasco, J. A. Encinar, and V. Losada, "Efficient numerical tool for the analysis and design of reflectarrays based on cells with three parallel dipoles," *Microw. Opt. Technol. Lett.*, vol. 55, no. 6, pp. 1212–1216, Jun. 2013.

[16] Á. F. Vaquero, M. Arrebola, M. R. Pino, R. Florencio, and J. A. Encinar, "Demonstration of a reflectarray with near-field amplitude and phase constraints as compact antenna test range probe for 5G new radio devices," *IEEE Trans. Antennas Propag.*, vol. 69, no. 5, pp. 2715–2726, May 2021.

[17] Á. F. Vaquero, "Development of techniques for the analysis and synthesis of spatially-fed arrays for emerging applications in near-field," Ph.D. dissertation, Ingeniería Eléctrica, Electrónica, de Computadores y Sistemas, Departamento de, Universidad de Oviedo, Oviedo, Spain, Nov. 2021.

[18] Á. F. Vaquero, M. R. Pino, and M. Arrebola, "Adaptive field-to-mask procedure for the synthesis of metalens antennas with complex near-field coverage patterns in 5G scenarios," *IEEE Trans. Antennas Propag.*, vol. 71, no. 9, pp. 7158–7171, Sep. 2023.

[19] A. Arboleya, Y. Álvarez, and F. Las-Heras, "Millimeter and submillimeter planar measurement setup," in *Proc. IEEE Antennas Propag. Soc. Int. Symp.*, Orlando, FL, USA, 2013, pp. 1–2.

[20] (Ticra, Copenhagen, Denmark). *TICRA: GRASP |Reflector Antenna Design Software*. Accessed: Nov. 17, 2022. [Online]. Available: http://www.ticra.com/software/grasp/

[21] Á. F. Vaquero, M. R. Pino, and M. Arrebola, "Dual-polarized shaped-beam transmitarray to obtain a multizone coverage for 5G indoor communicatiosn," *IEEE Antennas Wireless Propag. Lett.*, vol. 21, no. 4, pp. 730–734, Apr. 2022.

[22] (Ticra, Copenhagen, Denmark). *TICRA: SNIFT |Spherical Near-Field Far-Field Transformations*. Accessed: Nov. 27, 2022. [Online]. Available: http://www.ticra.com/software/snift/

[23] W. L. Stutzman and G. A. Thiele, *Antenna Theory and Design*, 3rd ed., Hoboken, NJ, USA: Wiley, 2012.

[24] R. G. Ayestarán, G. León, M. R. Pino, and P. Nepa, "Wireless power transfer through simultaneous near-field focusing and far-field synthesis," *IEEE Trans. Antennas Propag.*, vol. 67, no. 8, pp. 5623–5633, Aug. 2019, doi: 10.1109/TAP.2019.2916677.

[25] S. Yu, N. Kou, Z. Ding, and Z. Zhang, "Design of dual-polarized reflectarray for near-field shaped focusing," *IEEE Antennas Wireless Propag. Lett.*, vol. 20, no. 5, pp. 803–807, May 2021, doi: 10.1109/LAWP.2021.3063848.

[26] Á. F. Vaquero, R. Florencio, M. R. Pino, and M. Arrebola, "Dual-polarized near-field plane wave generator using an offset-optics reflectarray mm-wave band," *IEEE Trans. Antennas Propag.*, vol. 70, no. 12, pp. 12370–12375, Dec. 2022, doi: 10.1109/TAP.2022.3209176.

[27] S. Costanzo, F. Venneri, A. Borgia, and G. D. Massa, "Dual-band dual-linear polarization reflectarray for mmWaves/5G applications," *IEEE Access*, vol. 8, pp. 78183–78192, 2020, doi: 10.1109/ACCESS.2020.2989581.

[28] M. Arrebola, J. A. Encinar, and M. Barba, "Multifed printed reflectarray with three simultaneous shaped beams for LMDS central station antenna," *IEEE Trans. Antennas Propag.*, vol. 56, no. 6, pp. 1518–1527, Jun. 2008, doi: 10.1109/TAP.2008.923360.

ÁLVARO F. VAQUERO (Member, IEEE) was born in Salinas, Spain, in 1990. He received the B.Sc., M.Sc., and Ph.D. degrees in telecommunications engineering from the Universidad de Oviedo (UO), Gijón, Spain, in 2015, 2017, and 2021, respectively.

From 2016 to 2021, he was a Research Assistant with the Signal Theory and Communications Area, UO. He was a Visiting Researcher with the Antennas and Propagation Group, Instituto de Telecomuncações, Lisbon, Portugal, in 2017, 2021, and 2023. In December 2021, he joined the Department of Signals, Systems, and Radiocommunications, Group of Applied Electromagnetics, Universidad Politécnica de Madrid, Spain, as a Postdoctoral Researcher involved in the development of reflective intelligent surfaces for 5G/6G networks. He moved back to the University of Oviedo in 2022. He has authored more than 45 peer-reviewed journals and conference papers. His current research interest includes the development of efficient techniques for the analysis and optimization of spatially fed arrays, especially reflectarray, transmitarray, and metasurfaces for near- and far-field applications, the design of reconfigurable intelligent surfaces, and the design of additive manufacturing antennas in mm-wave frequencies.

Dr. Vaquero was a recipient of a Postdoctoral Fellowship financed by the Spanish Government in 2023. He has also received the 2022 Outstanding Ph.D. Thesis Award from UO and the 2021 National Award for the Best Ph.D. Thesis on Telecommunication Engineering for 5G Innovation for Sustainable Connectivity. He was also recipient of the IEEE Antennas and Propagation Society Fellowship in 2023.

BORJA IMAZ-LUEJE (Member, IEEE) was born in La Hueria, Spain, in 1995. He received the B.Sc., M.Sc., and Ph.D. degrees in telecommunication engineering from the Universidad de Oviedo (UO), Gijón, Spain, in 2017, 2019, and 2023, respectively.

Since 2016, he has been a Research Assistant with the Electrical Engineering Department, UO. From 2018 to 2019, he spent several months in Rohde & Schwarz GmbH & Co KG, Munich, Germany, where he was involved in the deployment of CATR systems and OTA measurements. In 2022, he was in a research mission with the Institut d'Electronique et des Technologies du numeRique, Rennes, France, where he was involved in the analysis and design of compact antennas. In 2023, he joined to the Department of Signal Theory and Communications and Telematic Systems and Computing, Universidad Rey Juan Carlos, Madrid, Spain, where he is currently an Assistant Professor. His current research interests include the development of efficient analysis and design techniques of reflectarrays in complex configurations, working in environments of near and far field.

MARCOS R. PINO received the M.Sc. and Ph.D. degrees in telecommunication engineering from the University of Vigo, Spain, in 1997 and 2000, respectively.

In 1998, he was a Visiting Scholar with the ElectroScience Laboratory, The Ohio State University, Columbus, OH, USA. From 2000 to 2001, he was an Assistant Professor with the University of Vigo. Since 2001, he has been with the Electrical Engineering Department, University of Oviedo, Gijón, Spain, where he is currently a Full Professor, teaching courses on communication systems and antenna design. From 2017 to 2023, he has spent several months as a Visiting Fellow with the Department of Information Engineering, University of Pisa, Italy, collaborating in near-field UHF-RFID applications. His current research interests include antenna design optimized for both near-field and far-field applications, antenna measurement techniques, and efficient computational techniques applied to EM problems.

MANUEL ARREBOLA (Senior Member, IEEE) was born in Lucena, Spain. He received the M.Sc. degree in telecommunication engineering from the University of Málaga, Málaga, Spain, in 2002, and the Ph.D. degree from the Technical University of Madrid (UPM), Madrid, Spain, in 2008.

From 2003 to 2007, he was a Research Assistant with the Department of Electromagnetism and Circuit Theory, UPM. He was a Visiting Researcher with the Department of Microwave Techniques, Universität Ulm, Ulm, Germany. In 2007, he joined the Department of Electrical Engineering, University of Oviedo, Gijón, Spain, where he is currently an Associate Professor with the Signal Theory and Communications Group. In 2009, he was with the European Space Research and Technology Center, European Space Agency, Noordwijk, The Netherlands, as a Visiting Researcher. He has been a Visiting Professor with several institutions, such as the Edward S. Rogers Sr. Department of Electrical and Computer Engineering, University of Toronto, Toronto, ON, Canada, in 2018; the Institute of Sensors, Signals and Systems, Heriot-Watt University, Edinburgh, U.K., in 2019; and the Antennas and Propagation Group, Instituto de Telecomuncações, Lisbon, Portugal, in 2023. He has authored and coauthored more than 200 peer-reviewed journals and conference papers. His current research interests include the application of innovative manufacturing techniques in mm and sub-mm-wave antenna design and the development of efficient analysis, design, and optimization techniques of spatial fed arrays, including reflectarrays and transmitarrays, and periodic structures for near- and far-field applications.

Dr. Arrebola was a co-recipient of the 2007 Sergei A. Schelkunoff Transactions Prize Paper Award from the IEEE Antennas and Propagation Society. He has also received the 2008 Outstanding Ph.D. Thesis Award from UPM and the 2009 National Award for the Best Ph.D. Thesis on Telecommunication Networks and Services. Since 2022, he has been an Associate Editor of the IEEE TRANSACTIONS ON ANTENNAS AND PROPAGATION and since 2024, he has been appointed as a Regional Delegate of the European Association on Antennas and Propagation.